Title
THE CROSS SECTION FOR COMPOUND-NUCLEUS FORMATION IN HEAVY-ION-INDUCED REACTIONS

Author
Thomas, T. Darrah.

Publication Date
1959-04-01

UCRL-695

UNIVERSITY OF CALIFORNIA

Ernest O. Lawrence

Radiation Laboratory

BERKELEY, CALIFORNIA

DISCLAIMER

UCRL-8695

UNIVERSITY OF CALIFORNIA
Lawrence Radiation Laboratory
Berkeley, California

Contract No. W-7405-eng-48

THE CROSS SECTION FOR COMPOUND-NUCLEUS FORMATION IN HEAVY-ION-INDUCED REACTIONS

T. Darrah Thomas

April 1959

Printed for the U. S. Atomic Energy Commission

THE CROSS SECTION FOR COMPOUND-NUCLEUS FORMATION IN HEAVY-ION-INDUCED REACTIONS*

T. Darrah Thomas

University of California
Lawrence Radiation Laboratory
Berkeley, California

April 1959

ABSTRACT

Compound-nucleus-formation cross sections for various systems of heavy ions and targets have been calculated by using two simple models. The first model, based on a square-well nuclear potential, gives reasonable agreement with experiment if a radius parameter $r_o \cong 1.5$ fermis is used. The second model, based on a diffuse nuclear potential, gives agreement if $r_o = 1.17$ fermis is used. The cross sections calculated by using the first model are presented for various energies of the systems carbon, nitrogen, oxygen, and neon incident on aluminum, potassium, copper, silver, praseodymium, gold, and uranium. Also tabulated are the average values of the orbital angular momentum for each system at each energy.

*Work done under the auspices of the U. S. Atomic Energy Commission.

THE CROSS SECTION FOR COMPOUND-NUCLEUS FORMATION IN HEAVY-ION-INDUCED REACTIONS

T. Darrah Thomas

University of California
Lawrence Radiation Laboratory
Berkeley, California

April 1959

INTRODUCTION

With the increasing availability of accelerators capable of producing beams of heavy ions (i.e., $Z > 2$) it has become useful to know the cross section for a heavy ion to form a compound nucleus by interaction with a target nucleus. The results of calculations based on two simple models are presented here in order to give some idea of the magnitude of this cross section as a function of the energy of the bombarding particle.

SQUARE-WELL MODEL

Assumptions

The assumptions of the first model used, which has been taken from Blatt and Weisskopf,[1] are as follows:

1. Both the target nucleus and the projectile nucleus are spheres having well-defined surfaces and radii, $R_i = r_o (A_i)^{1/3}$, where A_i is the mass number of the nucleus in question.

2. The real part of the potential energy of the system is given by

$$V = \frac{Z_1 Z_2 e^2}{r} + \frac{\hbar^2}{2\mu} \frac{\ell(\ell+1)}{r^2}, \quad \text{for } r > R_1 + R_2,$$

$$V = -\frac{\hbar^2 K_o^2}{2\mu}, \quad \text{for } r < R_1 + R_2,$$

$$K_o = 10^{13} \text{ cm}^{-1}.$$

Here Z_1 and Z_2 are the atomic number of target and projectile, r is the distance between the centers of the two particles, μ is the reduced mass of the system, and $\ell\hbar$ is the orbital angular momentum of the system.

3. There is an interaction radius, $R = R_1 + R_2$, such that for $r > R$ there is no nuclear interaction, and for $r < R$, there is a strong nuclear interaction causing the incident particle to be absorbed. Since incident particles with $r < R$ are not re-emitted, it is possible to represent the wave function of the incident particle within the nucleus as an incoming wave, i.e.,

$$u \sim e^{-iKr} \text{ for } r < R,$$

where K is the wave number of the particle inside the nucleus.

On the basis of these assumptions, the following formula is derived by Blatt and Weisskopf:

$$\sigma = \pi \lambda\!\!\!^{-2} \sum_{\ell=0}^{\infty} \frac{4 K R S_\ell}{\Delta_\ell^2 + (KR + S_\ell)^2} , \tag{1}$$

where

$$S_\ell = k R \frac{1}{F_\ell^2 + G_\ell^2} , \tag{2}$$

$$\Delta_\ell = k R \frac{F_\ell F_\ell' + G_\ell G_\ell'}{F_\ell^2 + G_\ell^2} , \tag{3}$$

$$K = (k^2 + K_o^2)^{1/2} ,$$

$$\lambda\!\!\!^{-} = \frac{1}{k} ,$$

$$F_\ell' = \frac{dF_\ell}{d(kr)} , \qquad G_\ell' = \frac{dG_\ell}{d(kr)}$$

F_ℓ and G_ℓ are Coulomb functions, and k is the wave number of the incident particle outside the nucleus. The Coulomb functions and their derivatives are evaluated for $r = R$.

Calculations

The calculations were performed on an IBM Type 650 computer. The method of Airy integrals and the Riccati 2 method described by Fröberg were used to evaluate the functions F_o, G_o, F_o', and G_o'.[2] Recursion formulas given by

Fröberg were used to calculate values of the Coulomb functions for $\ell > 0$. The summation of cross sections was continued until the last term was less than 0.01% of the sum already calculated.

Results

The results of calculations based on the model described are given in Tables I through VII for carbon, nitrogen, oxygen, and neon ions of a range of energies, incident on a variety of targets. Also given in these tables is the average value of the angular momentum, in units of $\hbar$, of the compound nucleus formed. The radius parameter, r_o, used in these calculations is 1.5 fermis. The results of some calculations using $r_o = 1.2$ fermis are given in Tables VIII and IX.

Comparison with Experiment

Comparisons of the calculated cross sections with experimentally determined ones are shown in Figs. 1-3. Figure 1 shows cross sections reported by Flerov for fission induced in uranium by different heavy ions.[3] It has been assumed that the cross section for fission is equal to the cross section for formation of the compound nucleus. Figure 2 shows the sum of fission and spallation cross sections measured by Flerov and co-workers for nitrogen-ion-induced reactions in gold.[4] In Figure 3, calculations for the system $K^{39}+N^{14}$ based on $r_o = 1.5$ and $r_o = 1.37$ are compared with experimental values reported by Pinajian and Halbert.[5]

Calculation of Cross Sections for Other Targets

In Fig. 4 is shown a plot for nitrogen-ion bombardments, of the quantity $\sigma/\pi R^2$ versus the quantity Z of the target. Curves for several values of ϵ/B are shown (ϵ is the center-of-mass energy of the system, B is the Coulomb barrier height). Graphs of this nature can be used to interpolate values of the cross section for systems that have not already been calculated. Similar but more

uncertain approximations can be made for different values of the radius parameter, r_o.

Angular Momentum of the Compound Nucleus

Figure 5 shows the cross section for a given value of the orbital angular momentum of the system, $\ell\hbar$, plotted against ℓ. Curves are given for three different energies of the system uranium plus carbon and four energies for the system aluminum plus carbon. In Figs. 6 and 7 are presented plots of the average orbital angular momentum versus laboratory-system energy of the particle for several systems. For the carbon-plus-uranium system and the carbon-plus-aluminum system curves based on a classical calculation are also shown. The average value of the orbital angular momentum is approximately equal to the average value of the total angular momentum of the compound nucleus.

DIFFUSE-WELL MODEL

Figures 1-3 indicate that the cross sections calculated by using the square-well model and a radius parameter of 1.5 fermis are not in bad agreement with the experimental values. Certainly the results based on $r_o = 1.5$ f are in far better agreement with experiment than those based on $r_o = 1.2$ f. Furthermore, experimentally determined cross sections for formation of a compound nucleus by alpha-particle bombardment are in agreement with values calculated by using the square-well model and a radius parameter of 1.5 fermis.[6]

It has been well established that the charge distribution of the nucleus does not correspond to a square well with a radius of $1.5\ A^{1/3}$ fermis, but rather to a diffuse well with a radius of the order of $1.2\ A^{1/3}$ fermis.[7] There is an apparent discrepancy between the radius parameter of ~1.5 fermis that must be used to get agreement between experiment and the calculations of the square-well model and the parameter of 1.2 fermis based on other evidence. This discrepancy is due in part to the dependence of the compound-nucleus formation cross section on the nuclear potential, which extends somewhat beyond the extent of the charge, and in part to the effects of the diffuse potential.

Let us consider a nuclear potential of the sort proposed by Igo for the alpha particle:[8]

$$V_n = -1100 \exp\left[-\left(\frac{r-1.17\,A^{1/3}}{0.574}\right)\right]. \qquad (4)$$

We may write, for any particle,

$$V_n = V_o \exp\left[-\left(\frac{r-1.17(A_1^{1/3} + A_2^{1/3})}{0.574}\right)\right]. \qquad (5)$$

If we set $1.17\,A_1^{1/3}$ equal to the root-mean-square radius of the alpha particle, 1.61 fermis,[9] we can show by comparison of Eq. (5) with Eq. (4) that $V_o = -67$ Mev.

The potential felt by a spherical charged particle near the nucleus can be written

$$V = \frac{Z_1 Z_2 e^2}{r} + \frac{\hbar^2}{2\mu}\frac{\ell(\ell+1)}{r^2} - 67 \exp\left[-\left(\frac{r-1.17(A_1^{1/3} + A_2^{1/3})}{0.574}\right)\right]. \qquad (6)$$

Figure 8 shows the diffuse potential for the gold-plus-carbon system for $\ell = 0$ and $\ell = 30$ compared with the square-well potential calculated for $r_o = 1.3$ f and $r_o = 1.5$ f. It can be seen that the maximum of the diffuse potential falls at a radius given by a radius parameter of between 1.3 f and 1.5 f.

Table X gives the radius at which the potential is a maximum for several systems, and also lists the value of r_o that would be necessary for this radius to be given by the formula $R = r_o (A_1^{1/3} + A_2^{1/3})$.

Table X. Radius at which the potential given by formula (6) is a maximum for various systems

System	Radius, R (fermis)	$r_o = R/(A_1^{1/3} + A_2^{1/3})$ (fermis)
U + N	11.70	1.36
Au + N	11.31	1.37
Pr + N	10.69	1.40
Ag + N	10.24	1.43
Cu + N	9.53	1.49
K + N	9.03	1.56
Al + N	8.75	1.62
N + N	9.02	1.87

If we consider this radius at which the potential has a maximum to be the interaction radius, then it is no longer surprising that such a large radius must be used with the square-well calculations.

To investigate the effects of the diffuse potential more quantitatively requires either elaborate calculations or some simplifying approximations. The approximation used here is that the total potential can be represented by a parabola that is matched in position, height, and curvature to the potential at its maximum. Two such parabolas are shown in Fig. 9.

The cross section for compound-nucleus formation is given as

$$\sigma = \pi \lambda\!\!\!^{-2} \sum_{\ell=0}^{\infty} (2\ell + 1)\, T_\ell, \tag{7}$$

where T_ℓ is the transmission coefficient for the ℓth partial wave. Hill and Wheeler have shown, for a parabolic potential,

$$T = \frac{1}{1 + \exp \frac{2\pi(B-E)}{\hbar\,\omega}}, \tag{8}$$

where B is the height of the barrier, E the energy of the system, and ω the vibrational frequency of the harmonic oscillator having a potential energy function given by the negative of the potential energy function describing the barrier.[9]

Results of calculations based on this model are compared in Fig. 10 with results based on the square-well model together with a radius parameter of 1.5 f and 1.2 f. The two cases shown represent the extremes of disagreement between the diffuse-well model and the square-well model with $r_o = 1.5$ f. It can be seen that, although a radius parameter of 1.17 f was used with the diffuse model, the agreement of the curves calculated is considerably better with the ones based on a square well and $r_o = 1.5$ f than with those based on a square well and $r_o = 1.2$ f.

COMPARISON WITH OPTICAL MODEL

Porter, using the optical model with a Woods-Saxon[10] type nuclear potential and a diffuseness parameter of 0.6 fermi, has calculated the compound-nucleus-formation cross section for the nitrogen-nitrogen system.[11] He used two sets of parameters: $r_o = 1.15$ fermis, real potential V = -40 Mev, imaginary potential W = -8 Mev; and $r_o = 1.25$ fermis, V = -20 Mev, W = -10 Mev. He shows that, for the $|V| \leq 10$ Mev, the real potentials given by these choices of parameters are essentially identical with an Igo-type potential (Eq. (5)) with $V_o = -36$ Mev. In Fig. 11 a comparison is made between his calculations (using a radius parameter of 1.15 fermis) and calculations based on the diffuse-well model described. The agreement, though not perfect, is surprisingly good.

Using the optical model and a potential that gives agreement with elastic scattering results, Igo has calculated total reaction cross sections for alpha particles incident on various targets.[12] The potential is

$$V_\alpha + i W_\alpha = -1100 \exp - \left(\frac{r-1.17 A^{1/3}}{0.574}\right) - i\, 45.7 \exp - \left(\frac{r-1.40 A^{1/3}}{0.578}\right) \text{ Mev}$$

for $|V_\alpha| \leq 10$ Mev. A comparison of these results, which are in good agreement with experiment, with those calculated by Blatt and Weisskopf using the square-well model, shows better agreement with those calculated using $r_o = 1.5$ fermis than with those calculated using $r_o = 1.3$ fermis. In fact, Igo's curves predict larger cross sections than are predicted by the square-well model with $r_o = 1.5$ fermis.

ACKNOWLEDGMENTS

I would like to express my thanks to Professor John O. Rasmussen for many helpful suggestions and to Miss Claudette Evenson and Miss Edna Williams for their assistance in running the IBM-650

REFERENCES

1. J. M. Blatt and V. F. Weisskopf, Theoretical Nuclear Physics (John Wiley and Sons, New York, 1952).
2. C. E. Fröberg, Revs. Modern Phys. 27, 399 (1955).
3. G. N. Flerov, Proceedings of the Conference on Reactions Between Complex Nuclei, Gatlinburg, 1958, ORNL-2606, Sept. 1958, p. 384.
4. Baraboshkin, Karamian, and Flerov, Zh. E. T. P., 1294 (1957).
5. J. J. Pinajian and M. L. Halbert, Phys. Rev. 113, 589 (1959).
6. Vandenbosch, Thomas, Vandenbosch, Glass, and Seaborg, Phys. Rev. 111, 1358 (1958).
7. Robert Hofstadter, Nuclear and Nucleon Scattering of High-Energy Electrons, Ann. Revs. Nuclear Sci. 7 (1957).
8. George Igo, Phys. Rev. Letters 1, 72 (1958).
9. D. L. Hill and J. A. Wheeler, Phys. Rev. 89, 1102 (1953).
10. R. D. Woods and D. S. Saxon, Phys. Rev. 95, 577 (1954).
11. C. E. Porter, Phys. Rev. 112, 1722 (1958).
12. George Igo, to be published.

Table I. Cross section for compound-nucleus formation, and average orbital angular momentum of the system, in heavy-ion bombardment of aluminum-27. (Square-well model; $r_0 = 1.5$ f)
(Numbers in parentheses indicate negative powers of 10; e.g., 6.31(1)=6.31x10^{-1})

E_{lab}	Bombarding ion: Carbon-12		Nitrogen-14		Oxygen-16		Neon-20	
(Mev)	σ(mb)	$\bar{l}(\hbar)$	σ(mb)	$\bar{l}(\hbar)$	σ(mb)	$\bar{l}(\hbar)$	σ(mb)	$\bar{l}(\hbar)$
14	6.31(1)	3.17						
16	10.1	3.56	6.10(2)	3.33				
18	57.7	4.22	1.40	3.61	4.59(3)	3.49		
20	156.	5.13	13.2	4.03	1.39(1)	3.70		
22	276.	6.13	58.0	4.71	1.93	3.99		
24	395.	7.09	142.	5.62	13.6	4.42		
26	504.	7.99	244.	6.61	51.9	5.10	1.44(2)	4.08
28			349.	7.57	122.	5.98	1.98(1)	4.30
30	693.	9.64	448.	8.48	210.	6.94	1.67	4.58
32			539.	9.33	303.	7.90	9.01	4.98
34					393.	8.82	31.6	5.56
35	863.	11.3	666.	10.6				
36					478.	9.68	75.9	6.33
38							138.	7.23
40	1007.	12.9	823.	12.2	635.	11.3	210.	8.16
42							285.	9.08
44							359.	9.97
45	1106.	14.2	964.	13.9	784.	13.0		
46							430.	10.8
48							498.	11.6
50	1193.	15.5	1063.	15.2	921.	14.6	561.	12.4
55	1260	16.7	1154.	16.5	1020.	16.0	706.	14.1
60	1318.	17.8	1224.	17.7	1114.	17.4	828.	15.8
65	1365.	18.8	1286.	18.9	1185.	18.6	933.	17.2
70	1406	19.8	1337.	19.9	1252.	19.8	1025.	18.6
75			1383.	20.9	1306.	20.8	1103.	19.9
80	1471.	21.6	1421.	21.9	1356.	21.9	1173.	21.1
85					1397.	22.9	1233.	22.2
90	1521	23.3	1485.	23.7	1436.	23.8	1288.	23.3

Table I (cont'd.)

E_{lab} (Mev)	Bombarding ion: Carbon-12 σ(mb)	Carbon-12 $\bar{\ell}(\hbar)$	Nitrogen-14 σ(mb)	Nitrogen-14 $\bar{\ell}(\hbar)$	Oxygen-16 σ(mb)	Oxygen-16 $\bar{\ell}(\hbar)$	Neon-20 σ(mb)	Neon-20 $\bar{\ell}(\hbar)$
95							1337.	24.3
100	1559.	24.8	1537.	25.4	1500.	25.6	1380.	25.3
105							1420.	26.3
110	1591.	26.3	1578.	26.9	1551.	27.3	1455.	27.2
115							1489.	28.1
120	1617.	27.6	1612.	28.4	1593.	28.9	1518.	29.0
130			1640.	29.8	1629.	30.4	1571.	30.6
140	1657.	30.2	1664.	31.2	1660.	31.8	1616.	32.2
150					1686.	33.1		
160			1703.	33.7	1709.	34.4	1687.	35.1
180							1744.	37.8
200							1787.	40.4

Table II. Cross section for compound-nucleus formation, and average orbital angular momentum of the system, in heavy-ion bombardment of potassium-39. (Square-well model; $r_o = 1.5$ f)
(Numbers in parentheses indicate negative powers of 10; e.g., 6.31(1)=6.31×10^{-1})

E_{lab}	Bombarding ion							
	Carbon-12		Nitrogen-14		Oxygen-16		Neon-20	
(Mev)	σ(mb)	$\bar{l}(\hbar)$	σ(mb)	$\bar{l}(\hbar)$	σ(mb)	$\bar{l}(\hbar)$	σ(mb)	$\bar{l}(\hbar)$
14	4.92(5)	3.34						
16	7.12(3)	3.54						
18	3.03(1)	3.80						
20	4.80	4.19						
22	32.1	4.82	2.56(1)	4.21				
24	103.	5.77	3.28	4.58	8.11(3)	4.31		
26	206.	6.88	20.9	5.16	1.70(3)	4.56		
28	318.	7.99	70.9	6.04	1.93	4.91		
30	427.	9.06	152.	7.12	12.2	5.42		
32	522.	9.95	247.	8.25	45.0	6.20	2.69(3)	4.90
34			345.	9.36	106.	7.22	4.24(2)	5.13
35	670.	11.5						
36			439.	10.4	185.	8.35	4.31(1)	5.41
38			526.	11.4	271.	9.48	2.90	5.79
40	847.	13.4	610.	12.3	358.	10.6	13.0	6.34
42			686.	13.2	442.	11.6	39.2	7.13
44			757.	14.0	521.	12.6	85.1	8.13
45	1005.	15.3	785.	14.3				
46					601.	13.6	146.	9.23
48							214.	10.4
50	1123.	16.9	940.	16.3	727.	15.1	285.	11.5
52							355.	12.5
54							424.	13.5
55	1220	18.3	1057.	18.0	878.	17.2		
56							490.	14.5
58							554.	15.4
60	1305	19.7	1160.	19.5	994.	18.9	620.	16.3
65	1372.	21.0	1248.	21.0	1101.	20.5	750.	18.3

Table II (cont'd.)

E_{lab}	Bombarding ion							
	Carbon-12		Nitrogen-14		Oxygen-16		Neon-20	
(Mev)	σ(mb)	$\bar{l}(\hbar)$	σ(mb)	$\bar{l}(\hbar)$	σ(mb)	$\bar{l}(\hbar)$	σ(mb)	$\bar{l}(\hbar)$
70	1433.	22.2	1320	22.3	1190.	22.0	873.	20.2
75	1483.	23.3	1386.	23.6			980.	22.0
80	1528.	24.4	1441.	24.8	1337.	24.8	1071.	23.5
85							1157.	25.1
90	1602.	26.5	1534.	27.1	1450.	27.2	1228.	26.5
100	1660.	28.4	1608.	29.1	1540.	29.5	1355.	29.1
110	1708.	30.2	1668.	31.1	1614.	31.6	1459.	31.6
120	1747.	31.8	1718.	32.9	1675.	33.6		
130	1780.	33.4			1726.	35.4	1618.	36.0
140	1807.	35.0	1795.	36.3	1770.	37.2		
150					1808.	38.9	1734.	39.9
160			1853.	39.4	1841.	40.5	1780.	41.7
170					1870.	42.1	1822.	43.4
180							1858.	45.1
190							1891.	46.7
200							1920.	48.3
225							1982.	52.0

Table III. Cross section for compound-nucleus formation, and average orbital angular momentum of the system, in heavy-ion bombardment of copper-63. (Square-well model; $r_o = 1.5$ f)
(Numbers in parentheses indicate negative powers of 10; e.g., 6.31(1), 6.31×10^{-1})

E_{lab}	Bombarding ion							
	Carbon-12		Nitrogen-14		Oxygen-16		Neon-20	
(Mev)	σ(mb)	$\bar{l}(\hbar)$	σ(mb)	$\bar{l}(\hbar)$	σ(mb)	$\bar{l}(\hbar)$	σ(mb)	$\bar{l}(\hbar)$
20	1.07(4)	4.19						
23	4.57(2)	4.55						
25			2.46(4)	4.70				
26	3.10	5.12						
28			5.01(2)	5.08				
29	42.4	6.25						
30					3.39(4)	5.17		
31			2.39	5.66				
32	161	8.05						
33					4.27(2)	5.55		
34			30.2	6.74				
35	315.	9.99						
36					1.63	6.12		
37			122.	8.51				
38	476.	11.8						
39					20.2	7.13	4.75(5)	5.87
40			255.	10.5				
41	620.	13.5						
42					88.9	8.82	4.71(3)	6.22
43			396.	12.4				
44	755.	15.0						
45					200.	10.8	1.89(1)	6.67
46			531.	14.2				
47	863.	16.3						
48					326.	12.8	3.29	7.36
49			655.	15.8				
50	976.	17.7						
51					450.	14.7	24.4	8.55

Table III (cont'd.)

E_{lab}	Bombarding ion							
	Carbon-12		Nitrogen-14		Oxygen-16		Neon-20	
(Mev)	σ(mb)	ℓ(h)	σ(mb)	ℓ(h)	σ(mb)	ℓ(h)	σ(mb)	ℓ(h)
52			764.	17.2				
54					568.	16.4	83.7	10.3
55	1121.	19.7	873.	18.7				
57					678.	18.0	174.	12.4
60	1247.	21.5	1020.	20.8	776.	19.5	276.	14.5
63							381.	16.4
65			1153.	22.8	928.	21.8		
66							482.	18.2
69							579.	19.9
70	1448.	24.8	1266.	24.7	1063.	23.9		
72							667.	21.4
75					1176.	25.8	759.	23.1
80	1598.	27.7	1447.	27.9	1277.	27.6	886.	25.3
85							1008.	27.5
90	1713.	30.3	1590.	30.9	1448.	30.9	1114.	29.5
100	1806.	32.7	1705.	33.6	1585.	33.9	1296.	33.2
110	1881.	34.9	1798.	36.1	1696.	36.7	1445.	36.5
120	1944.	37.1	1875.	38.4			1572.	39.6
130			1940.	40.6	1867.	41.7		
140	2041.	41.0	1996.	42.7			1771.	45.1
150			2044.	44.7	1993.	46.1		
160			2085.	46.6	2043.	48.2	1919.	50.0
170					2088.	50.2		
180					2127.	52.1	2035.	54.4
200					2194.	55.7	2128.	58.6
220							2203.	62.4

Table IV. Cross section for compound-nucleus formation, and average orbital angular momentum of the system, in heavy-ion bombardment of silver-107. (Square-well model; $r_o = 1.5$ f)
(Numbers in parentheses indicate negative powers of 10; e.g., 6.31(1)=6.31x10^{-1})

	Bombarding ion							
E_{lab}	Carbon-12		Nitrogen-14		Oxygen-16		Neon-20	
(Mev)	σ(mb)	$\bar{l}(\hbar)$	σ(mb)	$\bar{l}(\hbar)$	σ(mb)	$\bar{l}(\hbar)$	σ(mb)	$\bar{l}(\hbar)$
28	3.50(6)	5.12						
32	7.81(3)	5.59						
36	1.65	6.33	1.46(4)	5.91				
40	41.8	7.93	6.77(2)	6.48	1.95(6)	6.23		
44	188.	10.7	5.00	7.44	1.72(3)	6.69		
48	382.	13.5	61.8	9.50	2.88(1)	7.36		
52	575.	16.1	204.	12.5	10.2	8.59	4.39(7)	7.16
56	754.	18.5	377.	15.4	77.6	11.0	2.44(4)	7.60
60	912.	20.6	549.	18.1	211.	14.1	3.75(2)	8.20
64			709.	20.5	367.	17.1	1.74	9.14
65	1084.	23.0						
68			858.	22.8	522.	19.9	23.4	10.9
70	1242.	25.2						
72					668.	22.3	99.0	13.9
75			1084.	26.3				
76							215.	17.2
80	1493.	29.2	1222.	28.5	929.	26.8	345.	20.3
84							476.	23.2
85					1077.	29.4		
88							602.	25.8
90	1694.	32.7	1462.	32.6	1206.	31.7		
92							725.	28.3
96							833.	30.5
100	1851.	35.8	1652.	36.3	1428.	35.9	943.	32.8
105							1063.	35.3
110			1810	39.6	1613.	39.6	1176.	37.6
120	2092.	41.5			1768.	43.1	1378.	42.0
130			2053.	45.5			1550.	46.0
140	2261.	46.4			2012.	49.3		

Table IV (cont'd.)

E_{lab} (Mev)	Bombarding ion: Carbon-12 σ(mb)	Carbon-12 $\bar{\ell}(\hbar)$	Nitrogen-14 σ(mb)	Nitrogen-14 $\bar{\ell}(\hbar)$	Oxygen-16 σ(mb)	Oxygen-16 $\bar{\ell}(\hbar)$	Neon-20 σ(mb)	Neon-20 $\bar{\ell}(\hbar)$
150			2232.	50.8			1828.	53.1
160	2389.	50.9			2195.	54.8		
170			2367.	55.6			2041.	59.4
180					2338.	59.9		
190			2474.	60.0				
200					2452.	64.5	2282.	67.8
225					2565.	69.9		
250							2555.	79.8

Table V. Cross section for compound-nucleus formation, and average orbital angular momentum of the system, in heavy-ion bombardment of praseodymium-141. (Square-well model; $r_0 = 1.5$ f)
(Numbers in parentheses indicate negative powers of 10; e.g., 6.31(1)=6.31×10^{-1})

E_{lab}	Bombarding ion							
	Carbon-12		Nitrogen-14		Oxygen-16		Neon-20	
(Mev)	σ(mb)	$\bar{\ell}(\hbar)$	σ(mb)	$\bar{\ell}(\hbar)$	σ(mb)	$\bar{\ell}(\hbar)$	σ(mb)	$\bar{\ell}(\hbar)$
30	6.87(10)	5.40						
35	5.88(5)	5.86						
40	1.44(1)	6.58	1.06(6)	6.30				
45	18.5	8.12	5.04(3)	6.91	1.80(8)	6.72		
50	164.	11.5	1.79	7.93	1.44(4)	7.24		
55	400.	15.3	52.6	10.4	1.09(1)	8.03	3.48(12)	7.47
60	637.	18.7	222.	14.3	9.60	9.57	6.14(8)	7.89
65	849.	21.6	435.	18.1	97.6	12.9	1.46(4)	8.45
70	1047.	24.3	644.	21.6	271.	17.1	5.93(2)	9.27
75	1221.	26.8	836.	24.6	464.	21.0	4.43	10.7
80	1370.	29.1	1009.	27.4	652.	24.4	54.9	13.8
85			1171.	30.0	830.	27.6	181.	18.2
90	1627.	33.2	1314.	32.4	985.	30.4	338.	22.5
95					1133.	33.0	500.	26.4
100	1834.	36.8	1557.	36.6	1269.	35.5	657.	29.9
105							805.	33.1
110	2005.	40.2	1762.	40.5	1502.	40.0	946.	36.1
120	2147.	43.3	1931.	44.1	1702.	44.1	1192.	41.5
130					1870.	47.8	1410.	46.3
140	2371.	48.9	2201.	50.5	2017.	51.3	1596.	50.7
150	2460.	51.5	2308.	53.4	2143.	54.6	1762.	54.7
160					2254.	57.7	1906.	58.5
170			2486.	58.8				
180					2439.	63.4	2148.	65.4
200			2685.	66.0	2587.	68.6	2343.	71.7
225					2735.	74.7	2538.	78.8
250							2694.	85.4

Table VI. Cross section for compound-nucleus formation, and average orbital angular momentum of the system, in heavy-ion bombardment of gold-197.
(Square-well model; $r_o = 1.5$ f)
(Numbers in parentheses indicate negative powers of 10; e.g., 6.31(1)=6.31×10^{-1})

E_{lab}	Bombarding ion							
	Carbon-12		Nitrogen-14		Oxygen-16		Neon-20	
(Mev)	σ(mb)	$\bar{l}(\hbar)$	σ(mb)	$\bar{l}(\hbar)$	σ(mb)	$\bar{l}(\hbar)$	σ(mb)	$\bar{l}(\hbar)$
40	1.82(8)	6.30						
45	2.30(4)	6.81	1.26(11)	6.74				
50	2.06(1)	7.61	4.42(7)	7.17				
55	17.1	9.25	1.32(3)	7.76	5.89(10)	7.53		
60	145.	12.7	4.77(1)	8.70	4.70(6)	8.02		
65	364.	16.8	21.9	10.7	5.15(3)	8.70		
70	597.	20.5	142.	14.5	9.39(1)	9.79		
75	814.	23.6	335.	18.7	27.1	12.1	8.74(8)	9.07
80	1024.	26.8	542.	22.6	142.	16.2	1.10(4)	9.67
85	1205.	29.4	742.	26.1	315.	20.6	3.25(2)	10.5
90	1368.	31.9	932.	29.3	502.	24.7	2.31	11.9
95	1521.	34.2	1101.	32.1	684.	28.4	34.7	14.9
100	1660.	36.5	1257.	34.8	861.	31.7	137.	19.4
105			1405.	37.3	1019.	34.7	280.	24.1
110	1896.	40.5	1540.	39.7	1168.	37.5	437.	28.5
115					1310.	40.2	592.	32.5
120	2099.	44.2	1774.	44.0	1441.	42.8	743.	36.1
125							886.	39.4
130	2268.	47.6	1978.	48.0	1671.	47.4	1022.	42.5
135							1153.	45.5
140			2151.	51.7	1874.	51.7	1274.	48.3
150	2542	53.8	2303.	55.2	2049.	55.6	1494	53.4
160					2205.	59.3	1692.	58.1
170							1867.	62.5
175	2796.	60.7						
180					2464.	66.1	2025.	66.6
200							2294.	74.2
225							2564.	82.7
250			3156	82.2			2782.	90.5
279							2960.	97.6
300							3109.	104.

Table VII. Cross section for compound-nucleus formation, and average orbital angular momentum of the system, in heavy-ion bombardment of uranium-238. (Square-well model; r_o = 1.5 f)
(Numbers in parentheses indicate negative powers of 10; e.g., 6.31(1)=6.31x10^{-1})

E_{lab}	Bombarding ion							
	Carbon-12		Nitrogen-14		Oxygen-16		Neon-20	
(Mev)	σ(mb)	$\bar{\ell}(\hbar)$	σ(mb)	$\bar{\ell}(\hbar)$	σ(mb)	$\bar{\ell}(\hbar)$	σ(mb)	$\bar{\ell}(\hbar)$
40	6.38(14)	6.35						
45	1.11(8)	6.74						
50	1.05(4)	7.26						
55	9.17(2)	8.03	4.84(8)	7.58				
60	9.28	9.50	1.75(4)	8.14	1.13(11)	7.92		
65	107.	12.8	8.92(2)	8.96	1.33(7)	8.37		
70	310.	17.0	7.14	10.5	2.41(4)	8.97		
75	542.	20.9	82.1	13.8	8.23(2)	9.84	1.37(14)	8.97
80	768.	24.4	252.	18.2	5.51	11.4	1.80(10)	9.37
85	983.	27.7	455.	22.4	64.0	14.7	5.17(7)	9.88
90	1171.	30.5	659.	26.2	207.	19.3	3.67(4)	10.5
95	1350.	33.1	854.	29.7	385.	23.8	7.02(2)	11.5
100	1515.	35.7	1033.	32.8	571.	27.8	3.57	13.1
105					751.	31.5	41.6	16.4
110	1797.	40.2	1364	38.5	922.	34.9	146.	21.2
115					1086.	38.1	289.	26.2
120	2039.	44.3	1641.	43.4	1234.	40.9	443.	30.7
125							599.	34.8
130	2243.	48.1	1884.	47.9	1507.	46.2	750.	38.6
135							896	42.1
140					1746.	51.1	1034.	45.4
145							1168.	48.5
150	2573.	54.9	2274.	55.8	1955.	55.5	1292.	51.4
155							1409.	54.2
160					2140.	59.6	1521.	56.8
170							1729.	61.8
175	2881.	62.4	2639.	64.4	2379.	65.3		

Table VII (cont'd.)

E_{lab}	Bombarding ion							
	Carbon-12		Nitrogen-14		Oxygen-16		Neon-20	
(Mev)	σ(mb)	$\overline{\ell}(\hbar)$	σ(mb)	$\overline{\ell}(\hbar)$	σ(mb)	$\overline{\ell}(\hbar)$	σ(mb)	$\overline{\ell}(\hbar)$
180							1914.	66.5
200	3112.	69.1			2699.	73.8	2234.	74.9
225	3291.	75.2					2557.	84.3
250	3434.	80.8			3150.	88.5	2817.	92.8
275	3550.	86.1					3030.	100.6
300	3647.	91.1					3208.	107.9

Table VIII. Cross section for compound-nucleus formation, and average orbital angular momentum of the system, in heavy-ion bombardment of aluminum-27. (Square-well model; $r_o = 1.2$ f) (Numbers in parentheses indicate negative powers of 10; e.g., 6.31(1) = 6.31×10^{-1})

E_{lab}	Bombarding ion			
	Carbon-12		Neon-20	
(Mev)	σ(mb)	$\bar{l}(\hbar)$	σ(mb)	$\bar{l}(\hbar)$
16	1.17(1)	2.82		
18	1.52	3.04		
20	10.0	3.35		
22	36.7	3.82		
24	84.9	4.44		
26	146.	5.13		
28	209.	5.83		
30	270.	6.50		
32	327.	7.14	1.67(2)	3.80
34			1.21(1)	3.95
36			6.57(1)	4.14
38	469.	8.87	2.72	4.38
40	515.	9.43	8.70	4.69
42			21.8	5.11
44			43.7	5.64
45	589.	10.5		
46			73.5	6.24
48			109.	6.88
50	660.	11.6	146.	7.53
52			185.	8.18
54			224.	8.81
55	714.	12.6		
56			261.	9.42
58			297.	10.0
60	758.	13.5	332.	10.6
62			365.	11.1
65	799.	14.4	415.	12.0

Table VIII (cont'd.)

E_{lab} (Mev)	Bombarding ion: Carbon-12 σ(mb)	Carbon-12 $\bar{l}(\hbar)$	Neon-20 σ(mb)	Neon-20 $\bar{l}(\hbar)$
70	829.	15.2	483.	13.1
75	858.	16.0	540.	14.2
80	883.	16.7	600.	15.3
85			646.	16.3
90	923.	18.1	689.	17.2
95			730.	18.1
100	954.	19.4	762.	19.0
110	981.	20.6	824.	20.6
120	1001.	21.7	873.	22.1
130	1019.	22.8	915.	23.5
140	1034.	23.8	952.	24.8
150			983.	26.1
160			1010.	27.2
170			1034.	28.4
180			1055.	29.5
190			1074.	30.5
200			1090.	31.5
225			1125.	34.0

Table IX. Cross section for compound-nucleus formation, and average orbital angular momentum of the system, in heavy-ion bombardment of uranium-238. (Square-well model; $r_o = 1.2$ f) (Numbers in parentheses indicate negative powers of 10; e.g., 6.31(1) = 6.31×10^{-1})

E_{lab}	Bombarding ion			
	Carbon-12		Neon-20	
(Mev)	σ(mb)	$\overline{\ell}(\hbar)$	σ(mb)	$\overline{\ell}(\hbar)$
60	1.64(5)	6.62		
65	4.69(3)	7.08		
70	3.73(1)	7.76		
75	8.57	8.95		
80	56.2	11.2		
85	152.	14.1		
90	268.	17.0		
95	387.	19.6		
100	502	22.1	2.11(9)	8.83
105	608.	24.3	7.00(7)	9.20
110	716.	26.5	1.03(4)	9.66
115	807.	28.4	6.52(3)	10.3
120	899.	30.3	2.28(1)	11.1
125			3.43	12.3
130	1057.	33.7	22.1	14.6
135			68.0	17.8
140	1194.	36.9	134.	21.3
145			211.	24.6
150	1315.	39.8	290.	27.8
155			370.	30.7
160	1421.	42.5	448.	33.5
165			524.	36.1
170			596.	38.4
175			670.	40.9
180	1599.	47.5	735.	43.0
185			802.	45.2
190			863.	47.1
200	1742.	52.0	980.	51.0
210			1087.	54.6
225			1231.	59.6
250			1435.	67.1

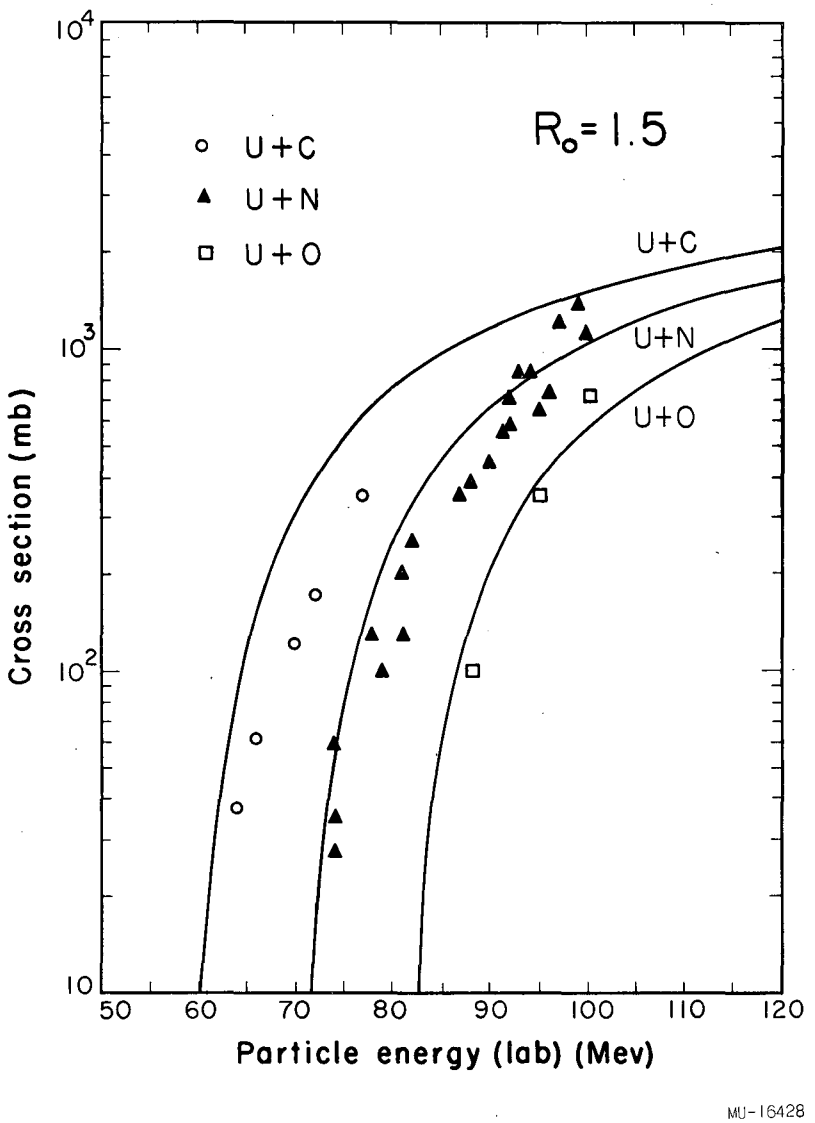

Fig. 1. Experimental values of the compound-nucleus-formation cross section compared with theoretical. Data from Flerov.[3]

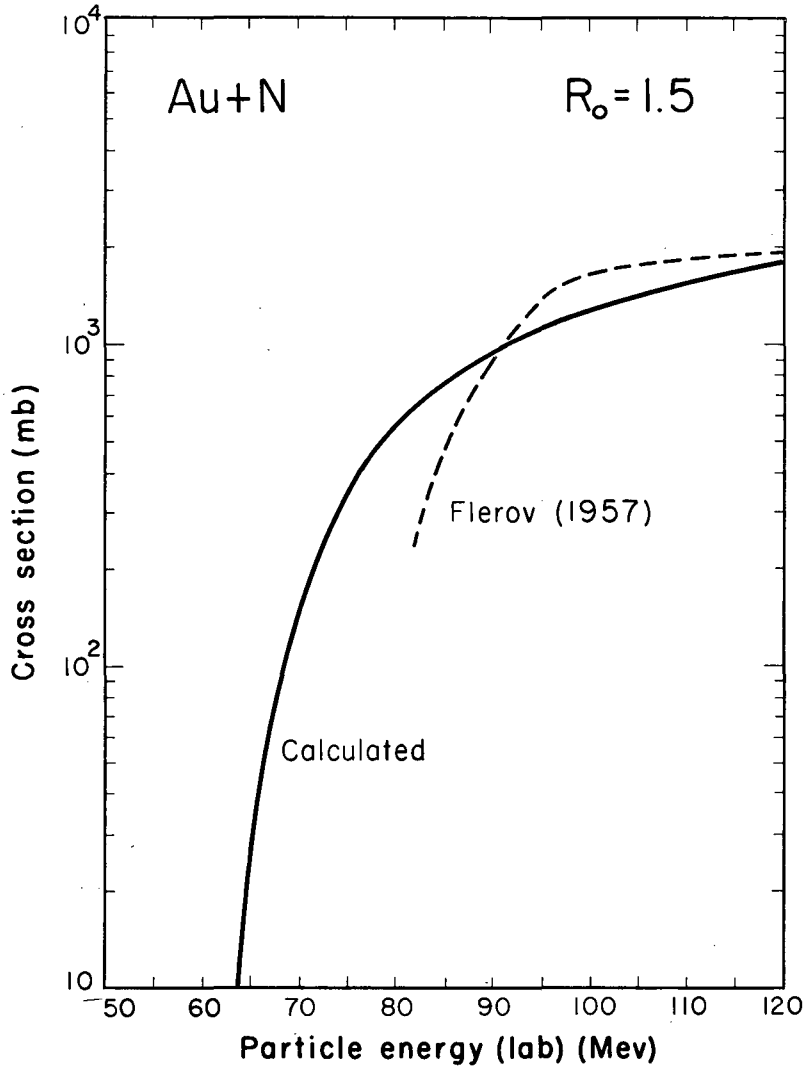

Fig. 2. Experimental values of the compound-nucleus-formation cross section compared with theoretical. Data from Baraboshkin et al.[4]

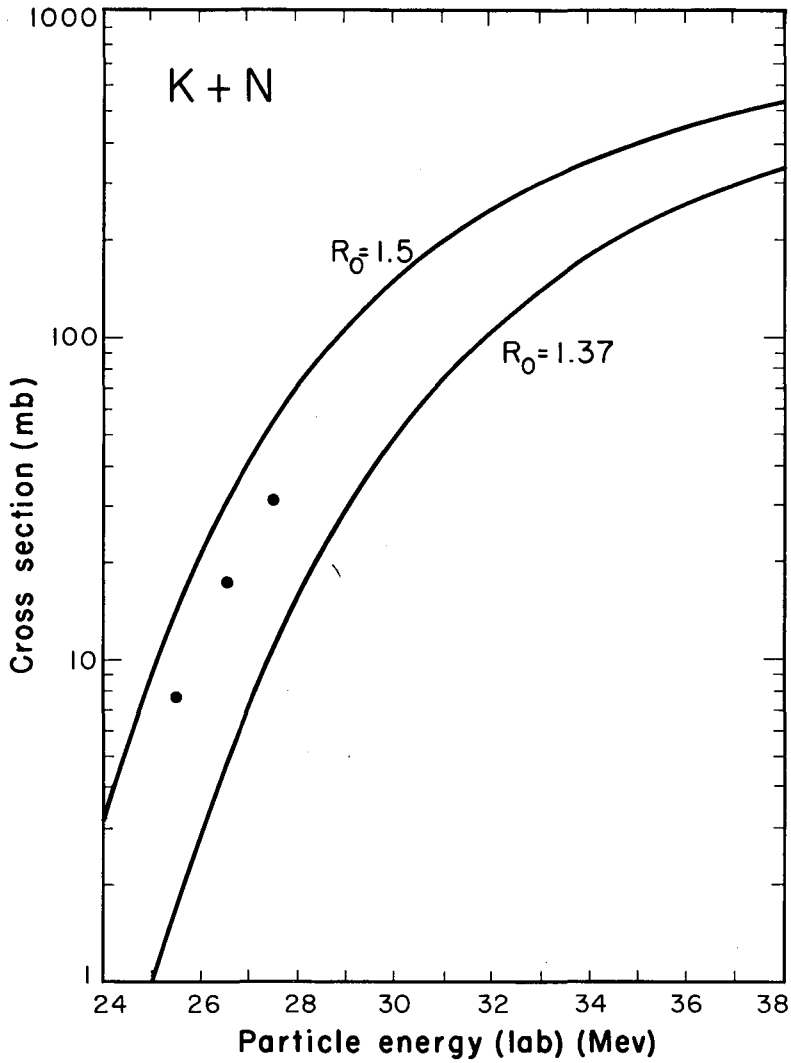

Fig. 3. Experimental values of the compound-nucleus-formation cross section compared with theoretical. Data from Pinajian and Halbert.[5]

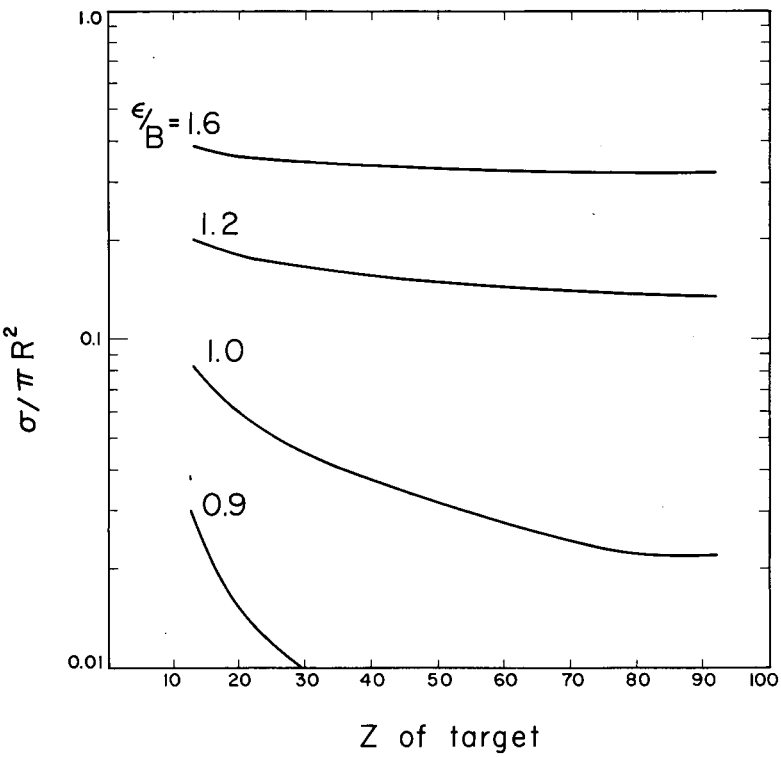

Fig. 4. $\sigma/\pi R^2$ plotted against Z of the target nucleus for nitrogen-ion bombardments for several values of the parameter ϵ/B. (ϵ is the center-of-mass energy, B is the Coulomb barrier height).

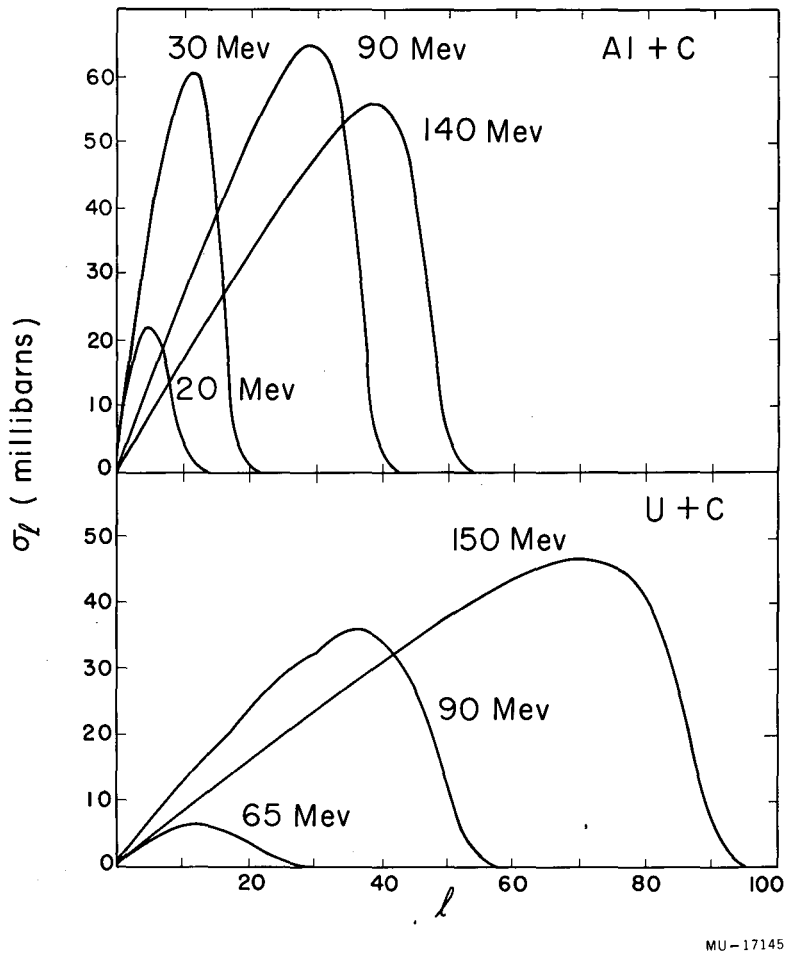

Fig. 5. σ_ℓ plotted against ℓ for uranium and aluminum plus carbon ions of different energies.

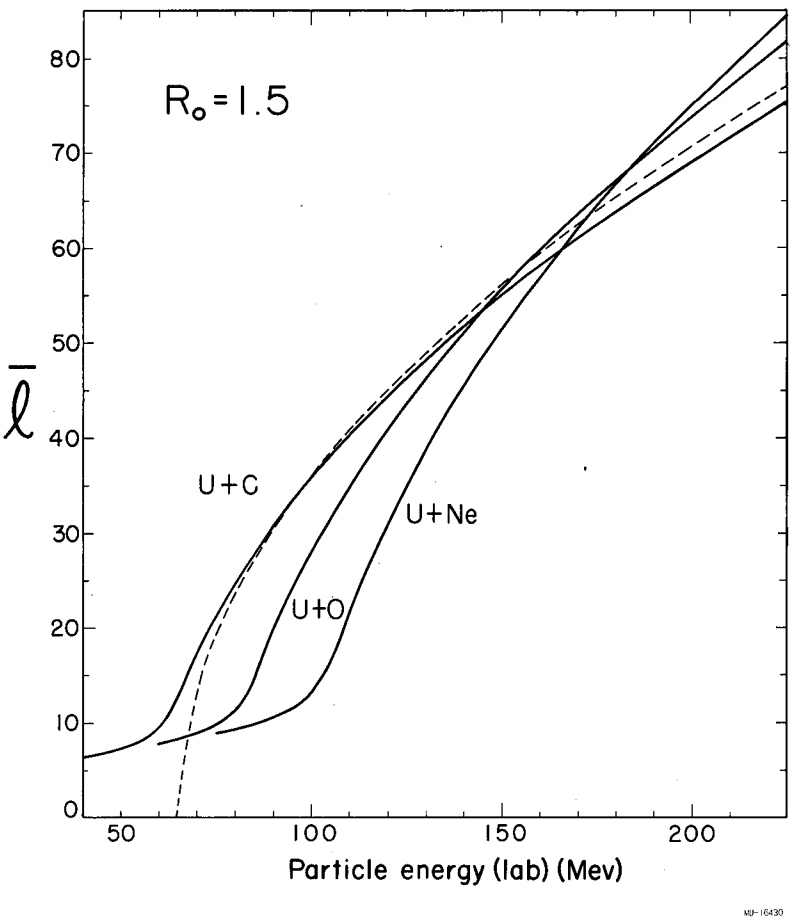

Fig. 6. Average orbital angular momentum as a function of energy for uranium plus various heavy ions. Dashed line is based on a classical calculation for uranium plus carbon.

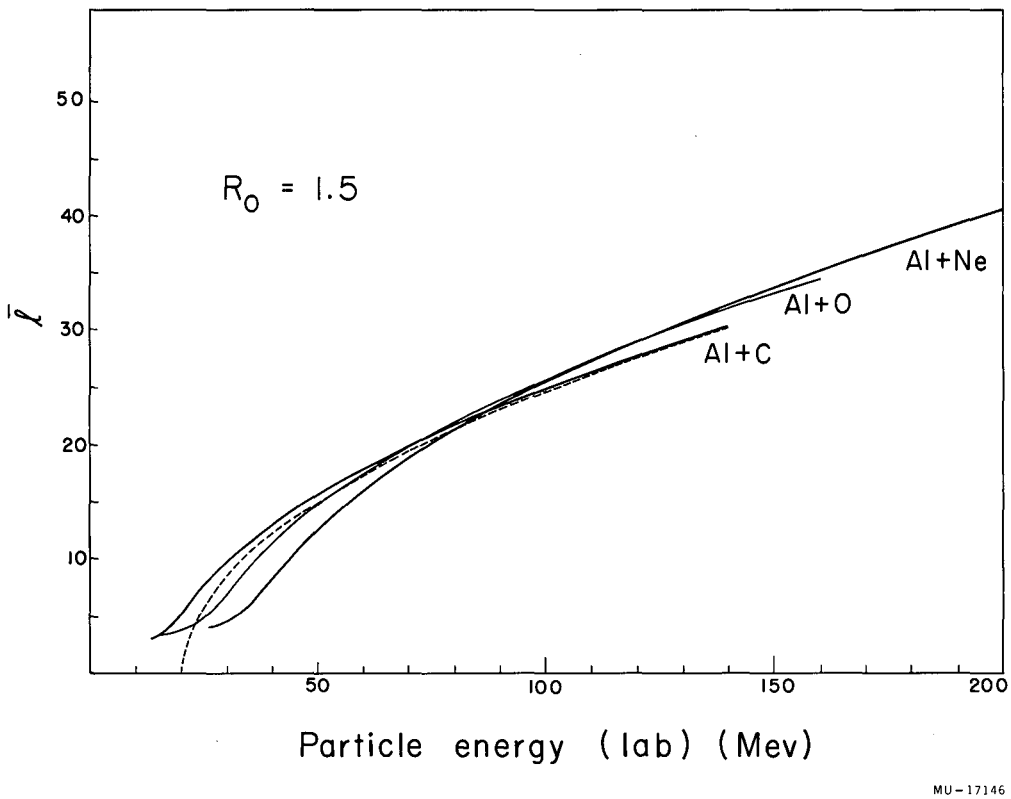

Fig. 7. Average orbital angular momentum as a function of energy for aluminum plus various heavy ions. Dashed line is based on a classical calculation for aluminum plus carbon.

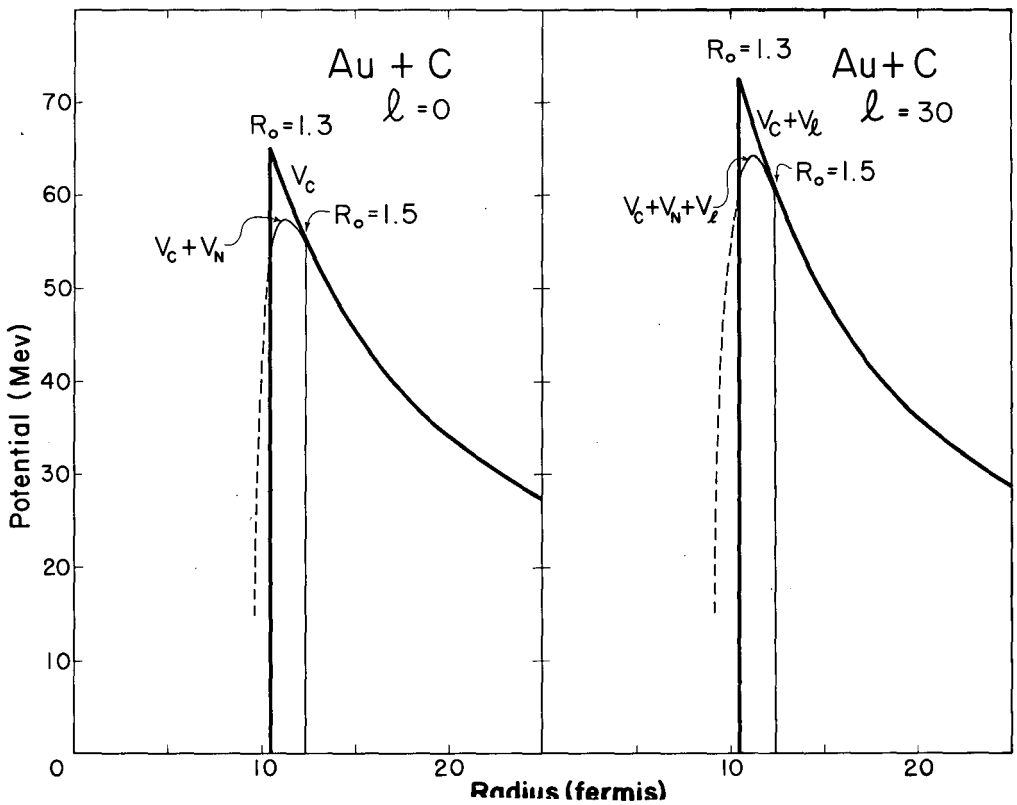

Fig. 8. Potential energy as a function of radius for the gold-plus-carbon system with $\ell = 0$ and $\ell = 30$. The square-well potential is compared with the diffuse-well potential.

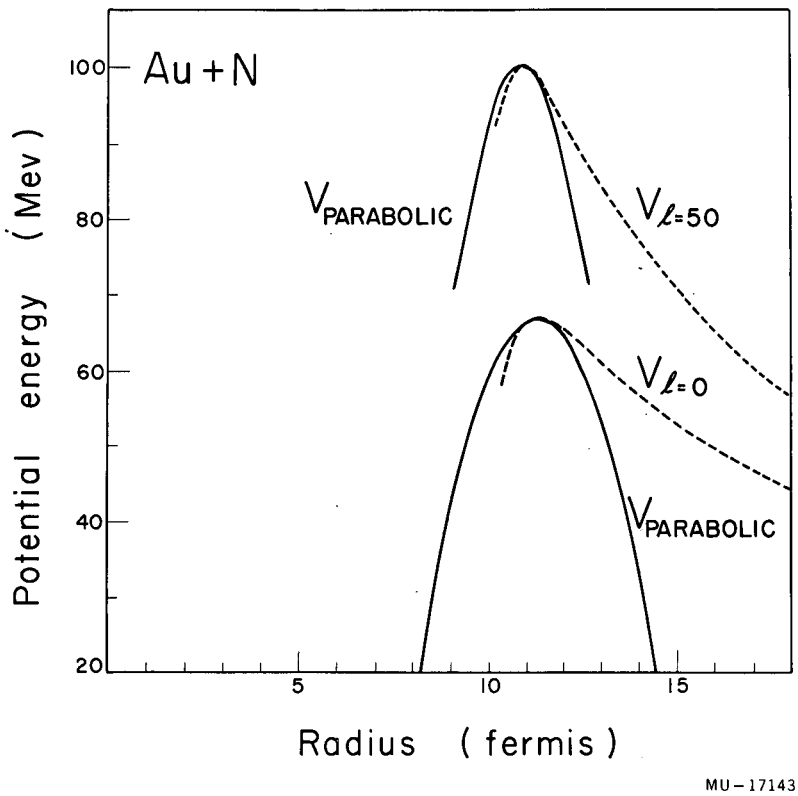

Fig. 9. Parabolas made to fit the diffuse-well potential at its maximum. For $\ell = 0$, $\hbar\omega$ is 5.58 Mev and for $\ell = 50$, $\hbar\omega$ is 7.95 Mev.

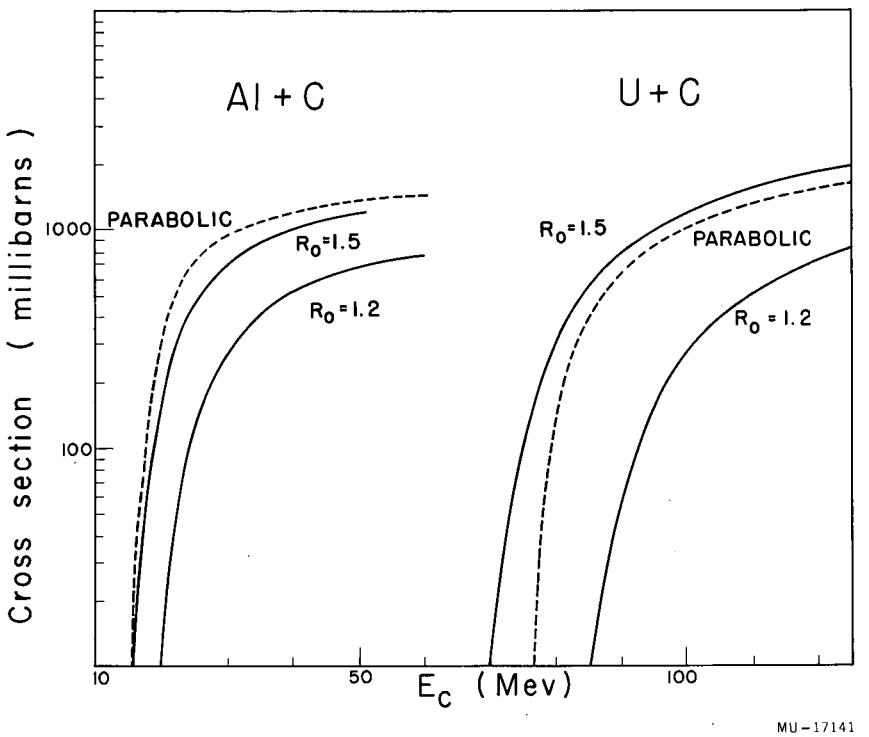

Fig. 10. Cross sections calculated by using the parabolic approximation to the diffuse-well potential compared with those calculated by using the square-well model and r_o = 1.5 fermis and r_o = 1.2 fermis.

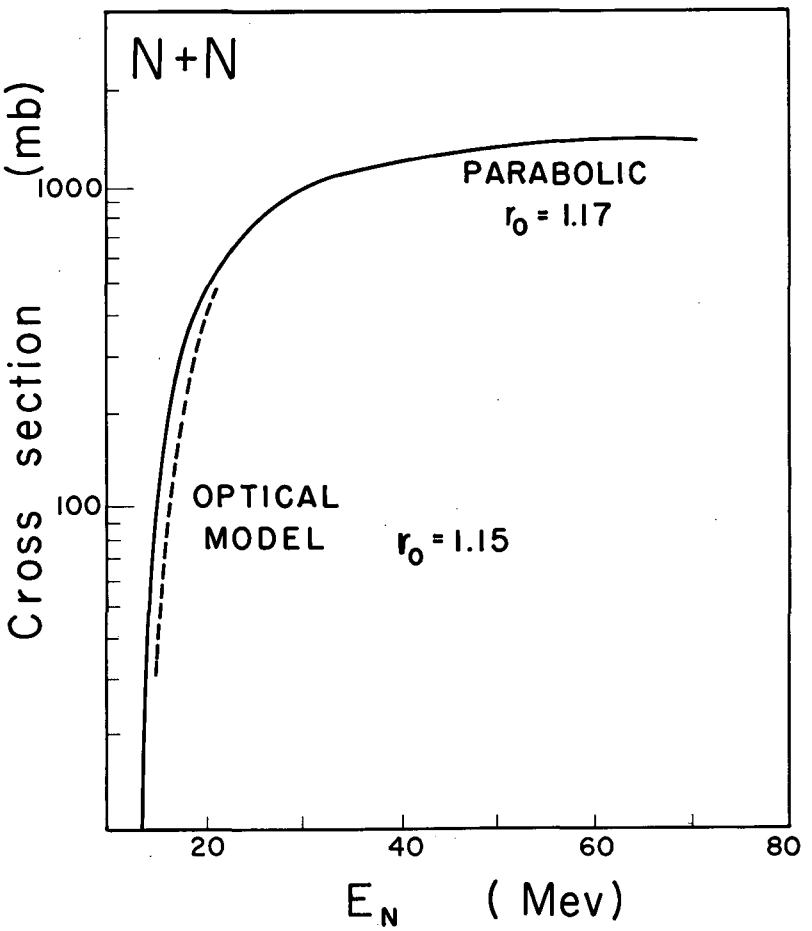

Fig. 11. Cross sections calculated by using the parabolic approximation to the diffuse-well potential compared with those calculated by Porter, using the optical model and a radius parameter of 1.15 fermis.[10]